

Gravitino dark matter and baryon asymmetry from Q -ball decay in gauge mediation

Shinta Kasuya^a and Masahiro Kawasaki^{b,c}

^a *Department of Information Sciences, Kanagawa University, Kanagawa 259-1293, Japan*

^b *Institute for Cosmic Ray Research, University of Tokyo, Chiba 277-8582, Japan*

^c *Institute for the Physics and Mathematics of the Universe, University of Tokyo, Chiba 277-8582, Japan*

(Dated: July 2, 2011)

We investigate the Q -ball decay in the gauge-mediated SUSY breaking. Q balls decay mainly into nucleons, and partially into gravitinos, while they are kinematically forbidden to decay into sparticles which would be cosmologically harmful. This is achieved by the Q -ball charge small enough to be unstable for the decay, and large enough to be protected kinematically from unwanted decay channel. We can then have right amounts of the baryon asymmetry and the dark matter of the universe, evading any astrophysical and cosmological observational constraints such as the big bang nucleosynthesis, which has not been treated properly in the literatures.

I. INTRODUCTION

Production of dark matter and baryon number of the universe is very important in cosmology. In the gauge-mediated supersymmetry (SUSY) breaking, the gravitino is natural candidate of the dark matter, while the Affleck-Dine (AD) baryogenesis [1] is promising mechanism because thermal leptogenesis confronts serious cosmological gravitino problem, for example. It is well known that the AD condensate transforms into nontopological solitons, Q balls, during the course of baryogenesis [2–6]. The charge of the Q ball in the gauge mediation could be large enough to be stable against the decay into nucleons, and the Q ball itself could be the dark matter of the universe [2]. In this case, however, nondetections in direct and/or indirect Q -ball searches tell us that it may be difficult to simultaneously obtain enough baryon asymmetry of the universe¹.

On the other hand, the small charge Q ball will decay into nucleons. At the same time, it could decay into gravitinos, which would have enough abundance to be the dark matter. This idea was considered in Refs.[7, 8]². In the former, the authors considered relatively small charge Q balls which evaporate in the thermal bath, and imagined that the gravitino is directly produced from the Q balls. In this case, however, most of the charge decays (evaporates) at the temperature around the electroweak scale, and sparticles are created, finally leading to the production of the next-to-lightest SUSY particle (NLSP), which thermalizes immediately. The gravitino could be produced by the NLSP decay, but the abundance of the gravitino is too small to be the dark matter of the universe, and the NLSP decay would destroy light elements during the big bang nucleosynthesis (BBN).

In the latter reference, the formed Q ball is the gravity-mediation type, which is able to decay into NLSPs non-thermally. The NLSP decays into the gravitino in the

end, but they did not discuss the fact that the NLSP abundance is limited severely by the BBN constraints for $m_{3/2} \gtrsim 1$ GeV, so that the amount of the produced gravitino should be much smaller than that to be the dark matter [9]³.

In this article, we investigate a very simple scenario that the unstable Q balls decay mainly into nucleons, partially into gravitinos with small branching ratio, while kinematically forbidden to NLSPs almost throughout the decay process, in the gauge-mediated SUSY breaking. The crucial observation reveals that the right amounts of the baryon asymmetry and the dark matter of the universe can be created through this process. The scenario is achieved by a couple of key ingredients. One is that the Q ball decays from its surface [11] so that the decay rate through the main channel has an upper bound, which is called the saturated rate, while the decay into gravitino is not saturated. Another is that a large enough Q ball forbids the decay into the NLSP, while allowing the decay into nucleons and gravitinos, having an appropriate lifetime to decay at the temperature of $O(10$ MeV).

The whole scenario proceeds as follows. The AD field starts the oscillation (rotation) after inflation. The rotation has an oblate orbit in the potential. Due to the negative pressure, the AD field feels spatial instabilities, which grow into Q and anti- Q balls. The Q and anti- Q balls decay into nucleons and anti-nucleons to create the baryon asymmetry in the universe, while producing small amount of gravitinos which become the dark matter of the universe. NLSPs would be produced only at the very end of the decay process when the charge of the Q ball becomes small enough to open the kinematically allowed channel to the NLSP production[12], and its abundance is small enough to evade any cosmological disasters such as spoiling the successful BBN.

The structure of the article is as follows. In the next section, we show the features of the Q ball in the gauge-mediated SUSY breaking model, and the details of the

¹ More recent observational limits tighter than those applied in Ref.[6] may wipe out the allowed regions.

² Its possibility was mentioned in Ref.[6].

³ Their model may work for a right-handed sneutrino LSP or if there is a small amount of R-parity violation[10].

decay process of the Q ball are described in Sec. III. In Sec. IV, we estimate the abundances of the baryon number, the dark matter, and the NLSP. We impose BBN constraints on the NLSP abundances to derive the allowed gravitino mass range in Sec. V. In Sec. VI, we show the region in the model parameter space where the successful scenario exists. Section VII is devoted to our conclusions.

II. Q BALL IN GAUGE MEDIATION

The AD field consists of some combination of squarks and sleptons. The potential is flat in the SUSY-exact limit, but due to the breaking of SUSY in gauge mediation, it is lifted as[13]

$$V(\Phi) = \begin{cases} m_\phi^2 |\Phi|^2, & (|\Phi| \ll M_S) \\ M_F^4 \left(\log \frac{|\Phi|^2}{M_S^2} \right)^2, & (|\Phi| \gg M_S) \end{cases}, \quad (1)$$

where $m_\phi \sim O(\text{TeV})$ is a soft breaking mass, and M_F and M_S are related respectively to the F and A components of a gauge-singlet chiral multiplet S in the messenger sector as

$$M_F^4 \equiv \frac{g^2}{(4\pi)^4} \langle F_S \rangle^2, \quad M_S \equiv \langle S \rangle. \quad (2)$$

Here g generically stands for the standard model gauge coupling, and M_F is allowed in the following range:

$$10^3 \text{ GeV} \lesssim M_F \lesssim \frac{g^{1/2}}{4\pi} \sqrt{m_{3/2} M_P}, \quad (3)$$

where $m_{3/2}$ is the gravitino mass and $M_P = 2.4 \times 10^{18}$ GeV is the reduced Planck mass.

The AD field starts the oscillation when $H \sim M_F^2/\phi_{\text{osc}}$, where ϕ_{osc} is the field amplitude at the onset of the oscillations. The field fluctuations grow exponentially due to the negative pressure during the helical motion, and the field transforms into Q balls. The charge of the formed Q ball is estimated as[6]

$$Q = \beta \left(\frac{\phi_{\text{osc}}}{M_F} \right)^4, \quad (4)$$

where $\beta \simeq 6 \times 10^{-4}$ for a circular orbit ($\varepsilon = 1$), while $\beta \simeq 6 \times 10^{-5}$ for an oblate case ($\varepsilon \lesssim 0.1$). Here ε represents the ellipticity of the field orbit. The charge Q is just the Φ -numbers, and relates to the baryon number of the Q ball as

$$B = bQ, \quad (5)$$

where b is the value of the baryon number carried by a Φ particle. For example, $b = 1/3$ for the udd direction. The mass, the size, the rotation speed of the field, and

the field value at the center of the Q ball are related to the charge Q as

$$M_Q \simeq \frac{4\sqrt{2}\pi}{3} M_F Q^{3/4}, \quad (6)$$

$$R_Q \simeq \frac{1}{\sqrt{2}} M_F^{-1} Q^{1/4}, \quad (7)$$

$$\omega_Q \simeq \sqrt{2}\pi M_F Q^{-1/4}, \quad (8)$$

$$\phi_Q \simeq M_F Q^{1/4}, \quad (9)$$

respectively.

III. Q-BALL DECAY

A Q -ball decay takes place if some decay particles carry the same kind of the charge of the Q ball, and the mass of all the decay particle is less than M_Q/Q . In this case, the Q -ball decay rate Γ_Q has an upper bound, which we call the saturated rate $\Gamma_Q^{(\text{sat})}$ [11]:

$$\Gamma_Q \lesssim \Gamma_Q^{(\text{sat})} \simeq \frac{1}{Q} \frac{\omega_Q^3}{192\pi^2} 4\pi R_Q^2 \simeq \frac{\pi^2}{24\sqrt{2}} M_F Q^{-5/4}, \quad (10)$$

where we use Eqs.(7) and (8) in the last equality. The decay rate saturates typically when $f_{\text{eff}}\phi_Q \gtrsim \omega_Q$, where the elementary process has an interaction of $\mathcal{L}_{\text{int}} = f_{\text{eff}}\phi\psi\bar{\psi}$. On the other hand, for $f_{\text{eff}}\phi_Q \ll \omega_Q$, the decay rate is given by[11]

$$\Gamma_Q \simeq 3\pi \frac{f_{\text{eff}}\phi_Q}{\omega_Q} \frac{1}{Q} \frac{\omega_Q^3}{192\pi^2} 4\pi R_Q^2 \simeq 3\pi \frac{f_{\text{eff}}\phi_Q}{\omega_Q} \Gamma_Q^{(\text{sat})}. \quad (11)$$

Since we are interested in the case that the Q ball can decay into nucleons ($M_Q/B > m_N$, where $m_N \simeq 1$ GeV is the nucleon mass) and, at the same time, the decay into NLSPs is kinematically prohibited ($M_Q/Q < m_{\text{NLSP}}$), the main decay channel is the decay into nucleons. We thus consider the Q -ball charge in the range $Q_{\text{cr}} < Q < Q_{\text{D}}$, where

$$Q_{\text{cr}} = \frac{1024\pi^4}{81} \left(\frac{M_F}{m_{\text{NLSP}}} \right)^4, \quad (12)$$

$$Q_{\text{D}} = \frac{1024\pi^4}{81} \left(\frac{M_F}{b m_N} \right)^4. \quad (13)$$

Notice that the NLSP is produced at the latest moment of the decay, only after the charge of the Q ball becomes less than Q_{cr} during the course of the decay[12].

The elementary process of the main channel is squark + squark \rightarrow quark + quark via (heavy) gluino exchange, whose rate is estimated as[14]

$$\Gamma_\phi \simeq \langle \sigma v \rangle n_\phi \simeq \frac{\zeta \alpha_s^2}{m_{\tilde{g}} \omega_Q} \omega_Q \phi_Q^2 \simeq \frac{1}{8\pi} \frac{\zeta g_s^4}{2\pi} \frac{\phi_Q^2}{m_{\tilde{g}} \omega_Q} \omega_Q, \quad (14)$$

where $m_{\tilde{g}}$ is the gluino mass, and $\zeta \sim |V_{\text{CKM}}|^4$ is a possible CKM suppression factor ($10^{-3} \lesssim |V_{\text{CKM}}| \lesssim 1$ [17]). Thus, we obtain the effective coupling as

$$f_{\text{eff}} \simeq \frac{\zeta^{1/2} g_s^2}{\sqrt{2\pi}} \frac{\phi_Q}{(m_{\tilde{g}} \omega_Q)^{1/2}}. \quad (15)$$

Since we have

$$\begin{aligned} \frac{f_{\text{eff}} \phi_Q}{\omega_Q} &\simeq 1.8 \times 10^{20} \zeta^{1/2} g_s^2 \left(\frac{M_F}{10^6 \text{ GeV}} \right)^{1/2} \\ &\times \left(\frac{m_{\tilde{g}}}{\text{TeV}} \right)^{-1/2} \left(\frac{Q}{10^{23}} \right)^{7/8} \gg 1, \end{aligned} \quad (16)$$

the main decay channel is saturated so that we must use the saturated rate $\Gamma_Q^{(\text{sat})}$ for the decay. Thus, the Q ball decays when the cosmic time becomes the lifetime of the Q ball: $t \simeq 1/\Gamma_Q^{(\text{sat})}$. The Q ball decays when the universe is radiation-dominated, and the cosmic temperature at the decay is estimated as

$$\begin{aligned} T_D &\simeq \left(\frac{90}{4\pi^2 N_*} \right)^{1/4} \sqrt{\Gamma_Q^{(\text{sat})}} M_P, \\ &\simeq 2.4 \text{ MeV} \left(\frac{M_F}{10^6 \text{ GeV}} \right)^{1/2} \left(\frac{Q}{10^{23}} \right)^{-5/8}, \end{aligned} \quad (17)$$

where N_* is the degrees of freedom at the corresponding temperature, and set to be 10.75 here.

On the other hand, the Q -ball decay into gravitinos is not saturated. The decay rate of the elementary process squark \rightarrow quark + gravitino is given by

$$\Gamma_{\phi \rightarrow q \psi_{3/2}} = \frac{1}{48\pi} \frac{m_\phi^5}{m_{3/2}^2 M_P^2}. \quad (18)$$

Since effective coupling is thus estimated as

$$f_{\text{eff}} \simeq \frac{1}{\sqrt{6}} \frac{\omega_Q^2}{m_{3/2} M_P}, \quad (19)$$

we have

$$\frac{f_{\text{eff}} \phi_Q}{\omega_Q} \simeq \frac{\pi}{\sqrt{3}} \frac{M_F^2}{m_{3/2} M_P} \lesssim \frac{\pi}{\sqrt{3}} \frac{g_s}{(4\pi)^2} \sim 0.01 g_s \ll 1, \quad (20)$$

where we use Eqs.(8) and (9) in the first equality, and Eq.(3) in the second equality. Therefore, the branching ratio of the decay into the gravitino is estimated as

$$B_{3/2} \equiv \frac{\Gamma_Q^{(3/2)}}{\Gamma_Q^{(\text{sat})}} \simeq 3\pi \frac{f_{\text{eff}} \phi_Q}{\omega_Q} \simeq \sqrt{3} \pi^2 \frac{M_F^2}{m_{3/2} M_P}. \quad (21)$$

IV. BARYON NUMBER, GRAVITINO DARK MATTER, AND NLSP ABUNDANCES

The number densities of the baryon number, the gravitino dark matter, and the NLSP are respectively related

to the number density of the AD field as

$$n_b \simeq \varepsilon b n_\phi, \quad (22)$$

$$n_{3/2} \simeq B_{3/2} n_\phi, \quad (23)$$

$$n_{\text{NLSP}} \simeq \frac{Q_{\text{cr}}}{Q} n_\phi. \quad (24)$$

WMAP seven-year data tells us $\rho_{\text{DM}}/\rho_b = 4.94_{-0.83}^{+0.95}$ [15]. Since the ratio of the gravitino dark matter and the baryon densities is

$$\frac{\rho_{3/2}}{\rho_b} = \frac{m_{3/2}}{m_N} \frac{n_{3/2}}{n_b} \simeq \frac{m_{3/2}}{m_N} \frac{B_{3/2}}{\varepsilon b} \simeq 5, \quad (25)$$

we must have

$$\varepsilon \simeq \frac{\sqrt{3}}{5} \pi^2 \frac{M_F^2}{m_{3/2} M_P} \frac{m_{3/2}}{b m_N} \simeq 1.4 \times 10^{-6} b^{-1} \left(\frac{M_F}{10^6 \text{ GeV}} \right)^2. \quad (26)$$

Therefore, the orbit of the AD field should be oblate, which is natural in the gauge-mediated SUSY breaking models. As mentioned above, this leads to the production of both Q and anti- Q balls to cancel out the baryon number to be small enough, compared to the gravitino dark matter.

Baryon number is created when the AD field starts the rotation. It can be estimated as

$$\begin{aligned} Y_b \equiv \frac{n_b}{s} &\simeq \frac{3}{4} T_{\text{RH}} \frac{n_b}{\rho_{\text{rad}}|_{\text{RH}}} \simeq \frac{3}{4} T_{\text{RH}} \frac{n_b}{\rho_{\text{inf}}|_{\text{osc}}} \\ &\simeq \frac{3}{4} T_{\text{RH}} \frac{\varepsilon b m_{\text{eff}} \phi_{\text{osc}}^2}{3 H_{\text{osc}}^2 M_P^2} \simeq \frac{9}{8\sqrt{2}} \frac{\varepsilon b \phi_{\text{osc}}^3 T_{\text{RH}}}{M_F^2 M_P^2}, \\ &\simeq \frac{9}{8\sqrt{2}} \varepsilon b \beta^{-3/4} \frac{M_F T_{\text{RH}}}{M_P^2} Q^{3/4}, \end{aligned} \quad (27)$$

where $m_{\text{eff}} \equiv \sqrt{|V''|} \simeq 2\sqrt{2} M_F^2/\phi_{\text{osc}}$ and $3H_{\text{osc}} \simeq m_{\text{eff}}$ are used in the last equality in the second line, and $\phi_{\text{osc}} = \beta^{-1/4} M_F Q^{-1/4}$ from Eq.(4) is used in the last line. Inserting Eq.(26), we obtain

$$\begin{aligned} \left(\frac{Y_b}{10^{-10}} \right) &\simeq 0.51 \left(\frac{\beta}{6 \times 10^{-5}} \right)^{-3/4} \left(\frac{T_{\text{RH}}}{10^6 \text{ GeV}} \right) \\ &\times \left(\frac{Q}{10^{23}} \right)^{3/4} \left(\frac{M_F}{10^6 \text{ GeV}} \right)^3. \end{aligned} \quad (28)$$

This provides the relation among Q , M_F , and T_{RH} .

On the other hand, the NLSP abundance is estimated as

$$\begin{aligned} \frac{\rho_{\text{NLSP}}}{s} &= m_{3/2} Y_{3/2} \frac{\rho_{\text{NLSP}}}{\rho_{3/2}}, \\ &\simeq 5 m_N Y_b \frac{m_{\text{NLSP}} n_{\text{NLSP}}}{m_{3/2} n_{3/2}}, \\ &\simeq 5 \frac{1024\pi^2}{81\sqrt{3}} m_N Y_b Q^{-1} \frac{M_F^2 M_P}{m_{\text{NLSP}}^3}, \\ &\simeq 3.2 \times 10^{-8} \text{ GeV} \left(\frac{Y_b}{10^{-10}} \right) \left(\frac{Q}{10^{23}} \right)^{-1} \\ &\times \left(\frac{M_F}{10^6 \text{ GeV}} \right)^2 \left(\frac{m_{\text{NLSP}}}{300 \text{ GeV}} \right)^{-3}, \end{aligned} \quad (29)$$

where $Y_{3/2} \equiv n_{3/2}/s$, and we use $\rho_{3/2}/\rho_b \simeq 5$ in the second equality, and Eqs.(23), (24), (12), and (21) in the third one. We can now consider the limits of the abundance from BBN constraints in the next section.

V. BBN CONSTRAINTS

The abundance of the NLSP is limited by BBN constraints, since the decay of the NLSP affects the abundances of light elements. It depends on the gravitino mass and the species of the NLSP how it has an influence on them. Let us first estimate the expected abundance of the NLSP in the limiting case, which means that the Q ball decays just in time for BBN ($T_D = 1$ or 3 MeV), and the thermally produced gravitinos do not overdominate. The latter condition is rephrased in terms of the constraint on the reheating temperature as[16]

$$T_{RH} \lesssim 3 \times 10^7 \text{ GeV} \left(\frac{m_{\tilde{g}_3}}{500 \text{ GeV}} \right)^{-2} \left(\frac{m_{3/2}}{\text{GeV}} \right), \quad (30)$$

where $m_{\tilde{g}_3}$ is a gluino mass evaluated at $T = T_{RH}$. Using Eqs.(17) and (28), we can eliminate M_F and Q from Eq.(29), which results in

$$\begin{aligned} \frac{\rho_{NLSP}}{s} &\simeq 7.0 \times 10^{-9} \text{ GeV} \left(\frac{T_{RH}}{10^6 \text{ GeV}} \right)^{-1/3} \\ &\times \left(\frac{T_D}{\text{MeV}} \right)^2 \left(\frac{m_{NLSP}}{300 \text{ GeV}} \right)^{-3}, \\ &\gtrsim 2.3 \times 10^{-9} \text{ GeV} \left(\frac{m_{3/2}}{\text{GeV}} \right)^{-1/3} \\ &\times \left(\frac{T_D}{\text{MeV}} \right)^2 \left(\frac{m_{NLSP}}{300 \text{ GeV}} \right)^{-3}, \end{aligned} \quad (31)$$

where Eq.(30) is used in the last inequality. In Fig.1, it is shown in red lines, above which is allowed. Also shown are the BBN constraints for bino (blue), stau (pink), and sneutrino (green) NLSPs, where upper right regions are excluded [9]. In addition, we plot the dotted line as the NLSP abundance that the gravitinos produced by the NLSP decay has a right amount of dark matter:

$$\begin{aligned} \left. \frac{\rho_{NLSP}}{s} \right|_{\max} &= m_{NLSP} Y_{3/2} \\ &= \frac{m_{NLSP}}{m_{3/2}} m_{3/2} Y_{3/2} \simeq \frac{m_{NLSP}}{m_{3/2}} 5 m_N Y_b \\ &\simeq 1.5 \times 10^{-7} \text{ GeV} \left(\frac{m_{NLSP}}{300 \text{ GeV}} \right) \\ &\times \left(\frac{m_{3/2}}{\text{GeV}} \right)^{-1} \left(\frac{Y_b}{10^{-10}} \right), \end{aligned} \quad (32)$$

Therefore, the NLSP abundance should be larger than the limit Eq.(31), and smaller than either excluded regions by BBN constraints in each NLSP species, or the upper limit that the produced gravitinos from the NLSP decay do not overclose the universe [Eq.(32)]. One can see that the gravitino mass above GeV is excluded. The

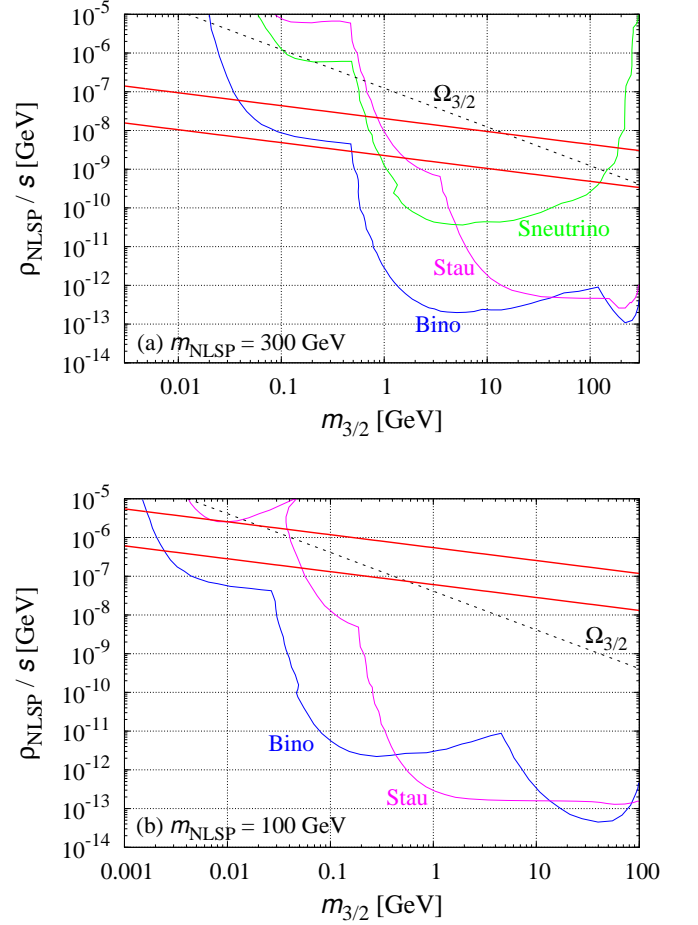


FIG. 1: NLSP abundance Eq.(31) for $T_D = 1$ (3) MeV, denoted as the lower (upper) red line, for (a) $m_{NLSP} = 300$ GeV and (b) $m_{NLSP} = 100$ GeV. BBN bounds are shown for bino (blue), stau (pink), and sneutrino (green, only in (a)), taken from Ref.[9]. Dotted line represents the upper bound of the abundance of NSLP that decays into gravitinos, above which overclose the universe [Eq.(32)]. The allowed abundance is in between the red line and BBN bounds or the dotted line.

allowed region is typically $m_{3/2} \lesssim \text{GeV}$ for $m_{NLSP} = 300$ GeV, and $m_{3/2} \lesssim 10^{-2} \text{ GeV}$ for $m_{NLSP} = 100$ GeV. The detail will be found in Table I.

VI. SUCCESSFUL SCENARIO

As shown in the previous section, the allowed parameter space is restricted by BBN constraints severely, but there is still a good chance to have successful scenario. Here we estimate the allowed region in Q -ball parameters, namely in $Q - M_F$ plane.

Equation (28) tells us the iso- T_{RH} lines in $Q - M_F$ plane, which reads

$$Q \simeq 2.4 \times 10^{23} \left(\frac{T_{RH}}{10^6 \text{ GeV}} \right)^{-4/3} \left(\frac{M_F}{10^6 \text{ GeV}} \right)^{-4}. \quad (33)$$

TABLE I: Upper limit of $m_{3/2}$ in GeV.

		$T_D = 1 \text{ MeV}$	$T_D = 3 \text{ MeV}$
300 GeV	bino	0.48	3.9×10^{-2}
300 GeV	stau	1.6	0.86
300 GeV	sneutrino	0.91	0.66
100 GeV	bino	2.5×10^{-3}	1.9×10^{-3}
100 GeV	stau	5.3×10^{-2}	2.1×10^{-2}

In the same manner, we can obtain iso-NLSP density lines from Eq.(29) as

$$Q \simeq 3.2 \times 10^{23} \left(\frac{\rho_{\text{NLSP}}/s}{10^{-8} \text{ GeV}} \right)^{-1} \times \left(\frac{M_F}{10^6 \text{ GeV}} \right)^2 \left(\frac{m_{\text{NLSP}}}{300 \text{ GeV}} \right)^{-3}, \quad (34)$$

and iso- T_D lines from Eq.(17) as

$$Q \simeq 4.0 \times 10^{23} \left(\frac{T_D}{\text{MeV}} \right)^{-8/5} \left(\frac{M_F}{10^6 \text{ GeV}} \right)^{4/5}. \quad (35)$$

Upper limit of the reheating temperature depends on the gravitino mass $m_{3/2}$ in such a way as in Eq.(30), and once we fixed $m_{3/2}$ we can restrict the NLSP abundances from Fig.1. Therefore, for the fixed $m_{3/2}$, the allowed region is above the line (33) with the largest possible T_{RH} , and between the lines (34) with the lower and upper NLSP abundances. In addition, the Q ball must decay before the BBN time so that the temperature at the decay T_D should be larger than 1 MeV (or 3 MeV for more conservative limit), represented as line (35).

We plot these lines for $m_{\text{NLSP}} = 300 \text{ GeV}$ in $Q - M_F$ planes in Fig.2 for $m_{3/2} = 1 \text{ GeV}$, 0.1 GeV, 0.01 GeV, and 1 MeV. Red lines denote the T_D contours, light blue lines are the T_{RH} contours, and dark green lines represent the NLSP abundance contours. Also shown in blue are the mass per charge M_Q/Q lines:

$$Q \simeq 1.2 \times 10^{27} \left(\frac{M_F}{10^6 \text{ GeV}} \right)^4 \left(\frac{M_Q/Q}{\text{GeV}} \right)^{-4}, \quad (36)$$

above which is prohibited for the Q ball to decay into those particles with mass larger than M_Q/Q . In particular, the Q -ball decay with baryon number is stable above the upper blue line denoted by $M_Q/(bQ) = 1 \text{ GeV}$ [equivalent to Eq.(13)], and the 300 GeV NLSP is only produced once the charge of the Q ball becomes below the lower line denoted as $M_Q/Q = 300 \text{ GeV}$ [equivalent to Eq.(12)].

Only the stau NLSP is allowed in the region shown in faint red in Fig.2(a). In Fig.2(b), there are three territories, where the faint ($T_D > 1 \text{ MeV}$) and the dark ($T_D > 3 \text{ MeV}$) red are applicable to the stau and the sneutrino NLSPs, while the blue is for the bino NLSP. On the other

hand, all three species (bino, stau, and sneutrino NLSPs) are relevant for the allowed region in Fig.2(c), which corresponds to the NLSP abundance between the red lines [Eq.(31)] and the dotted line [Eq.(32)] in Fig.1(a). We can see in Fig. 2(d) where $m_{3/2} = 1 \text{ MeV}$ that the allowed region disappear completely for $T_D > 3 \text{ MeV}$, and only a tiny area remains for $T_D > 1 \text{ MeV}$. Thus, we obtain the lower bound of the gravitino mass that could result in successful scenario as $m_{3/2} \gtrsim 1.1 \times 10^{-3} (6.9 \times 10^{-4}) \text{ GeV}$ for $T_D > 3 (1) \text{ MeV}$.

Notice that the allowed regions reside in such parameter space that the Q -ball charge is by far large enough so that the Q ball survives from the evaporation in thermal bath, where the Q ball evaporates if the charge is less than [6]

$$Q_{\text{evap}} \simeq 2.3 \times 10^{16} \left(\frac{M_F}{10^6 \text{ GeV}} \right)^{-4/11} \left(\frac{m_\phi}{\text{TeV}} \right)^{-8/11}, \quad (37)$$

which is shown by green dashed lines in Fig.2. On the other hand, black dotted lines in these figures denote the boundary above which the Q ball is the gauge-mediation type:

$$Q_{\text{gauge}} \simeq 10^{12} \left(\frac{M_F}{10^6 \text{ GeV}} \right)^4 \left(\frac{m_\phi}{\text{TeV}} \right)^{-4}. \quad (38)$$

Also notice that those Q balls in the allowed region in Fig. 2(a) ($m_{3/2} = 1 \text{ GeV}$) will form when the field starts rotation at the field amplitude larger than $\sim M_F^2/m_{3/2}$, where the gravity-mediation effects dominate over the gauge-mediation ones. Depending on the one-loop potential, the formed Q ball could be the delayed type [6] or the new type [18] which later transforms into the gauge-mediation type, or the gauge-mediation type may form directly.

VII. CONCLUSIONS

We have investigated the scenario of simultaneous production of the baryon asymmetry and the dark matter of the universe through the Q -ball decay in the gauge-mediated SUSY breaking model. This is simply achieved by the Q ball with charge small enough to decay into nucleons to create baryon number of the universe. We have calculated the branching ratio of the gravitino to find that it is small. Therefore, in order to obtain the observed baryon to dark matter abundance ratio, the AD field should rotate in the oblate orbit so that both Q and anti- Q balls are created to suppress the baryon number compared to the gravitino dark matter.

At the same time, the charge should be large enough to kinematically forbid the decay into NLSPs. This evades the serious BBN constraints on the NLSP abundance, which was not properly taken into account in the literatures. NLSPs are actually produced at the very end of the Q -ball decay when the charge becomes small enough to open the corresponding decay channel.

Including all these considerations, we have used the BBN constraints for the bino, stau, and sneutrino NLSPs in Ref.[9], to get the allowed range of the gravitino mass. We have found that typically $m_{3/2} \lesssim 1$ (10^{-2}) GeV for $m_{\text{NLSP}} = 300$ (100) GeV.

We have also shown the allowed region in $Q - M_F$ plane for $m_{\text{NLSP}} = 300$ GeV. We thus have found the production of right amounts of both the baryon asymmetry and the gravitino dark matter of the universe is successful when the Q ball has the charge $Q \simeq 10^{23}$ for $M_F \simeq 10^6 - 10^7$ GeV and $m_{3/2} \simeq 10^{-2} - 10^{-1}$ GeV. It is naturally achieved, for example, for the $n = 6$ udd direction. In this case, the nonrenormalizable superpotential $W_{\text{NR}} = (udd)^2/M_{\text{P}}^3$ determines the field amplitude at the onset of the oscillation $\phi_{\text{osc}} \simeq (M_F^2 M_{\text{P}}^3)^{1/5}$, and also leads

to the A -term of the form $V_A \sim am_{3/2}W_{\text{NR}} + \text{h.c.}$, and the scenario is successful for $M_F \sim 10^7$ GeV, $m_{3/2} \sim 0.01$ GeV, and $a \sim 0.1$, which leads to $\phi_{\text{osc}} \sim 7 \times 10^{13}$ GeV, and $Q \sim 10^{23}$.

Acknowledgments

The work is supported by Grant-in-Aid for Scientific Research 23740206 (S.K.), 14102004 (M.K.) and 21111006 (M.K.) from the Ministry of Education, Culture, Sports, Science and Technology in Japan, and also by World Premier International Research Center Initiative (WPI Initiative), MEXT, Japan.

-
- [1] I. Affleck and M. Dine, Nucl. Phys. B **249**, 361 (1985).
 - [2] A. Kusenko and M. E. Shaposhnikov, Phys. Lett. B **418**, 46 (1998).
 - [3] K. Enqvist and J. McDonald, Phys. Lett. B **425**, 309 (1998); Nucl. Phys. B **538**, 321 (1999).
 - [4] S. Kasuya and M. Kawasaki, Phys. Rev. D **61**, 041301(R) (2000).
 - [5] S. Kasuya and M. Kawasaki, Phys. Rev. D **62**, 023512 (2000).
 - [6] S. Kasuya and M. Kawasaki, Phys. Rev. D **64**, 123515 (2001).
 - [7] I. M. Shoemaker and A. Kusenko, Phys. Rev. D **80**, 075021 (2009).
 - [8] F. Doddato and J. McDonald, arXiv:1101.5328 [hep-ph].
 - [9] M. Kawasaki, K. Kohri, T. Moroi and A. Yotsuyanagi, Phys. Rev. D **78**, 065011 (2008).
 - [10] J. McDonald, private communication; F. Doddato and J. McDonald, arXiv:1107.1402.
 - [11] A. G. Cohen, S. R. Coleman, H. Georgi and A. Manohar, Nucl. Phys. B **272**, 301 (1986).
 - [12] S. Kasuya and F. Takahashi, JCAP **0711**, 019 (2007).
 - [13] A. de Gouvêa, T. Moroi and H. Murayama, Phys. Rev. D **56**, 1281 (1997).
 - [14] J. R. Ellis, J. S. Hagelin, D. V. Nanopoulos, K. A. Olive and M. Srednicki, Nucl. Phys. B **238**, 453 (1984).
 - [15] N. Jarosik *et al.*, Astrophys. J. Suppl. **192**, 14 (2011).
 - [16] M. Kawasaki, F. Takahashi and T. T. Yanagida, Phys. Rev. D **74**, 043519 (2006).
 - [17] K. Nakamura *et al.* [Particle Data Group], J. Phys. G **37**, 075021 (2010).
 - [18] S. Kasuya and M. Kawasaki, Phys. Rev. Lett. **85**, 2677 (2000).

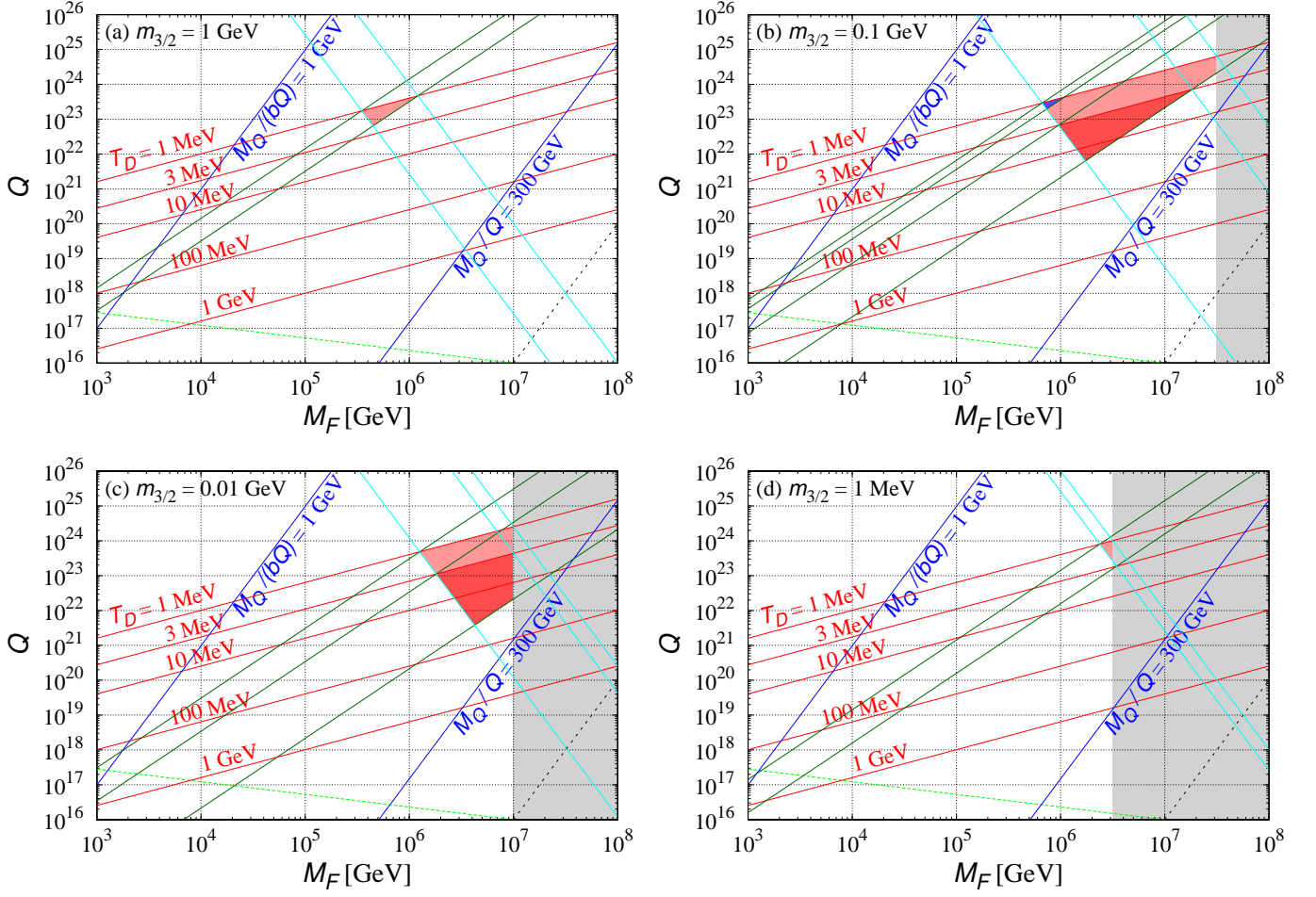


FIG. 2: Allowed region in $Q - M_F$ plane for (a) $m_{3/2} = 1$ GeV, (b) $m_{3/2} = 0.1$ GeV, (c) $m_{3/2} = 0.01$ GeV, and (d) $m_{3/2} = 1$ MeV. In all figures, red lines denote iso- T_D contours from 1 MeV to 1 GeV from the top to the bottom, and blue lines denote the limit of the mass of the particle which the Q ball can decay into: the upper is for nucleons and the lower is for the 300 GeV NLSP. Here we take $b = 1/3$. Gray hatched region is out of the range of M_F [Eq.(3)].

(a) Only the stau NLSP has allowed region. Light blue lines represent the T_{RH} contours for $T_{RH} = 3 \times 10^7$ GeV (the lower) and 3.5×10^5 GeV (the upper). The upper and lower dark green lines indicate $\rho_{NLSP}/s = 2.3 \times 10^{-9}$ GeV and 1.0×10^{-8} GeV, respectively.

(b) The faint and the dark red regions are applicable to the stau and the sneutrino NLSPs for $T_D > 1$ MeV and $T_D > 3$ MeV, respectively, while the bino NLSP is only allowed in the blue region. Light blue lines represent the T_{RH} contours for $T_{RH} = 3 \times 10^6$ GeV (the lower), 74 GeV (the middle), and 2.7 GeV (the upper). The dark green lines indicate $\rho_{NLSP}/s = 4.9 \times 10^{-9}$ GeV, 8.8×10^{-9} GeV, 4.4×10^{-8} GeV, and 1.5×10^{-6} GeV, from the top to the bottom, respectively.

(c) The faint and the dark red regions are applicable to all the NLSP species for $T_D > 1$ MeV and $T_D > 3$ MeV, respectively. Light blue lines represent the T_{RH} contours for $T_{RH} = 3 \times 10^5$ GeV (the lower), 64 GeV (the middle), and 17 GeV (the upper). The dark green lines indicate $\rho_{NLSP}/s = 1.0 \times 10^{-8}$ GeV, 9.4×10^{-8} GeV, and 1.5×10^{-5} GeV, from the top to the bottom, respectively.

(d) Allowed region is applicable to all the NLSP species. Light blue lines represent the T_{RH} contours for $T_{RH} = 3 \times 10^4$ GeV (the lower) and 1×10^4 GeV (the upper). The upper and lower dark green lines indicate $\rho_{NLSP}/s = 2.3 \times 10^{-8}$ GeV and 2.0×10^{-7} GeV, respectively.

In all figures, green dashed line shows the limit of the charge evaporated in thermal bath, and Q ball is the gauge-mediation type above the black dotted line.